

## Tracer Chromatographic Study of Pore and Pore Mouth Adsorption of Linear and Monobranched Alkanes on ZSM-22 Zeolite

Refik A. Ocakoglu,<sup>†</sup> Joeri F. M. Denayer,<sup>\*,†</sup> Guy B. Marin,<sup>‡</sup> Johan A. Martens,<sup>§</sup> and G. V. Baron<sup>†</sup>

*Dienst Chemische Ingenieurstechniek, Vrije Universiteit Brussel, Pleinlaan 2, B-1050 Brussel, Belgium, Laboratorium voor Petrochemische Techniek, Universiteit Gent, Krijgslaan 281, B-9000 Gent, Belgium, and Centrum voor Oppervlaktechemie en Katalyse, Katholieke Universiteit Leuven, Kasteelpark Arenberg 23, B-3001 Leuven, Belgium*

*Received: July 8, 2002; In Final Form: October 28, 2002*

The adsorption equilibria of a series of *n*-alkanes and 2-methyl- and 3-methyl-branched alkanes in the C<sub>5</sub>–C<sub>9</sub> range on ZSM-22 zeolite samples were determined using the tracer chromatographic technique at temperatures between 343 and 623 K. Adsorption experiments were performed with a calcined ZSM-22 sample referred to as “open” ZSM-22 and an as-synthesized ZSM-22 zeolite sample in which the 1,6-diaminohexane template was left inside the pores, denoted as “closed” ZSM-22. In the “open” ZSM-22, the zeolite micropores are available for adsorption. In the “closed” ZSM-22, adsorption can occur in the pore mouths and on the external surface. The closing of the channels of ZSM-22 results in a significant decrease in the Henry constant and adsorption enthalpy and entropy of linear alkane molecules. Contrarily, the adsorption enthalpy and entropy of branched alkanes on “open” and “closed” ZSM-22 are nearly identical, indicating that the preferred adsorption sites for monobranched alkanes are not located inside the pores, but specifically at the entrance of the pore. For the pore mouth adsorption mode, a characteristic compensation between adsorption enthalpy and entropy was observed. The entropy losses upon adsorption inside the narrow ZSM-22 channels are much larger than in channel openings. These data support the pore mouth catalysis model for alkane hydro-isomerization on ZSM-22 type catalysts.

### Introduction

Separation and isomerization of alkane skeletal isomers are very important processes in petroleum refining. Isomerization of linear alkanes into their branched isomers results in an improvement of the gasoline octane number and the low-temperature properties of aviation fuels<sup>1,2</sup> and are essential to the synthesis of lubricants. Isoalkanes are also feedstocks for alkylation processes yielding multibranched alkanes for gasoline octane boosting. Industrially, three types of heterogeneous catalysts are used to convert linear alkanes into branched ones: chlorinated alumina, sulfated zirconia, and noble metal loaded zeolite catalysts.<sup>3–7</sup> The isomerization of *n*-alkanes proceeds through a well-known chemistry, in which the linear chains are first transformed into monobranched alkanes, and subsequently into isomers with several branches.<sup>7,8</sup> The branched alkanes are very sensitive to undesirable cracking reactions.

Zeolites, with their well-defined pore structures and pore diameters close to those of the alkane molecules, are suitable adsorbents and catalysts for alkane separation and transformation purposes. Eight-ring zeolites such as the 5A type are currently used as molecular sieves to separate linear alkanes from branched alkanes.<sup>9–11</sup> For catalytic *n*-alkane hydroisomerization processes, ten-ring zeolites such as ZSM-22 (having a TON framework type) with their constrained tubular channel system

have the optimal pore shape and size to suppress undesired cracking reactions.<sup>12</sup> Undulating channels surrounded by ten-membered rings with a free diameter of 0.55 × 0.45 nm run through the TON framework in only one crystallographic direction. Channel intersections are absent on ZSM-22.<sup>13</sup>

Among the 10-membered ring zeolites, ZSM-22 is found to be the most selective zeolite catalyst for the conversion of *n*-alkanes in 2-methyl-branched isoalkanes.<sup>2,14</sup> This peculiarity of ZSM-22 in isomerization of *n*-alkanes into 2-methyl-branched isomers has been explained in various ways. One line of reasoning is that the transition state required for the formation of a branching near the end of the carbon chain is more slender than those for central branching of the chain, the formation of which is sterically suppressed.<sup>15,16</sup> Modeling of adsorption and diffusion of the isoalkanes in zeolite models with TON type framework led to the suggestion of product diffusion selectivity.<sup>14,16</sup> A third explanation proposes that the catalytic transformations of *n*-alkanes occur specifically in the pore openings, with the molecule only partially inside the confinement of the pore. The branching is created in the first lobe of the pore.<sup>1,17,18</sup> The deeper the *n*-alkane penetrates into the pore, the stronger the interaction, explaining the preference for branching at carbon atoms near the end of the chain.

There is a general agreement in the literature that linear alkanes have access to the pores and that double branched alkanes with the two branches on the same carbon or on neighboring carbon atoms are too bulky to enter and diffuse inside the channels of ZSM-22.<sup>8,15,19,20</sup> Pieterse et al.<sup>19</sup> studied the sorption of dibranched alkane molecules on TON type zeolites using microcalorimetry and gravimetry. They showed

\* Corresponding author. E-mail: Joeri.Denayer@vub.ac.be. Fax: +32 2 629 32 48.

<sup>†</sup> Vrije Universiteit Brussel.

<sup>‡</sup> Universiteit Gent.

<sup>§</sup> Katholieke Universiteit Leuven.

that the 2,2-dimethyl-branched molecules adsorb at low coverages parallel to the outer surface and, as the coverage increases, a linear part penetrates inside the pore. Concerning the adsorption and diffusion of monobranched isoalkanes, theory and experiments lead to different interpretations. Maesen et al.<sup>15</sup> calculated the adsorption properties of normal and branched alkanes on ZSM-22 using a configurational-bias Monte Carlo approach and suggested that the branched alkanes with only one methyl group are able to enter the TON type pores. Molecular dynamics calculations were further used by Webb et al.,<sup>21</sup> who arrived at 1–2 orders of magnitude lower diffusion constants for 2-methyl monobranched alkanes compared to linear ones, and an additional lowering by about 1 order of magnitude when the position of the methyl branching is moved from carbon position 2 to 3. Adsorption and diffusion simulations by Raybaud et al.<sup>8</sup> were in line with those of Webb et al. A molecular dynamics study by Corma et al.<sup>16</sup> revealed 4 times higher self-diffusion constants for *n*-heptane compared to 2-methylhexane at 450 K. Anderson et al.<sup>22,23</sup> used the positron emission profiling technique to investigate adsorption/diffusion behavior of alkanes on a packed bed of ZSM-22. The experimental data showed that micropore diffusion did not play a major role in the mass transport through the bed.

The adsorption equilibria of a range of linear and branched alkanes on ZSM-22 at catalytically relevant temperatures were determined using tracer and perturbation chromatographic techniques.<sup>24</sup> Branched alkanes were found to have significantly lower Henry adsorption constants and adsorption enthalpies than linear alkanes. The enthalpies could be very well explained by a combination of an interaction of one part of the molecule inside the pore and an interaction of the other part of the molecule with the external surface.<sup>25</sup> The division of the molecule between in and out of the pore is at the tertiary carbon atom.

In the present work, adsorption properties of linear and monobranched alkanes were studied on a normal open form and on a ZSM-22 sample, the pores of which were closed by leaving the organic template inside after synthesis and using only gentle activation at low temperature. According to the pore mouth adsorption model, this should have a dramatic impact on the adsorption of linear alkanes, whereas the impact on branched alkanes should be limited.

## Experimental Procedures and Materials

Zeolite ZSM-22 was synthesized according to the recipe of Ernst et al.<sup>13</sup> The synthesis starts from an aluminosilicate hydrogel containing potassium and 1,6-diaminohexane. The “closed” ZSM-22 sample corresponds to the as-synthesized form. It was experienced that the sample can be pretreated at 230 °C without desorption of template. To obtain the “open” ZSM-22, the as-synthesized sample was pelletized into 250–500  $\mu\text{m}$  particles, loaded as a packed bed into a quartz tube, and carbonized under flowing nitrogen at 400 °C using a heating ramp of 5 °C/min. After 5 h at 400 °C, the gas stream was switched to oxygen and the temperature increased to 550 °C, where it was kept for 16 h. The sample was cooled and ammonium exchanged at reflux conditions in 0.5 M  $\text{NH}_4\text{Cl}$  solution. Deammoniation was done by calcinations at 400 °C. Micropore volume and specific external surface area of open and closed ZSM-22 determined with nitrogen porosimetry are given in Table 1. For the closed ZSM-22, the *t*-plot external surface area approximately equals the BET surface area (44.3 to 46.06  $\text{m}^2/\text{g}$ ), whereas on the open ZSM-22, the BET surface area equals 256  $\text{m}^2/\text{g}$ . This demonstrates that the pores of the

TABLE 1: Adsorbent and Column Properties

	open ZSM-22	closed ZSM-22
BET surface area ( $\text{m}^2/\text{g}$ )	255.6	46.06
<i>t</i> -plot surface area ( $\text{m}^2/\text{g}$ )	48.5	44.3
<i>t</i> -plot micropore volume ( $\text{mL/g}$ )	$95.7 \times 10^{-3}$	$0.16 \times 10^{-3}$
Si/Al	30	30
column length (m)	0.35	0.35
adsorbent mass (g)	0.655	0.569
$\epsilon_{\text{ext}} + \epsilon_{\text{macr}}$	0.75	0.77
temp range (K)	343–503	473–623

closed ZSM-22 are not accessible to the  $\text{N}_2$  molecules and that only the external surface is available for adsorption.

The zeolite powders were compacted into disks by applying a pressure of ca. 30 MPa, and the disks were broken into fragments and sieved. For open ZSM-22 the 400–500  $\mu\text{m}$  and for the closed form of ZSM-22 the 250–400  $\mu\text{m}$  fraction were filled into a  $1/8$  in. diameter stainless steel column with a length of 0.35 m. This column was placed in a HP-4890 gas chromatograph (GC) equipped with a thermal conductivity detector (TCD) detector.

In situ activation of the adsorbents was performed by raising the temperature from ambient to 110 °C at a rate of 1 °C/min and maintaining the temperature for 30 min, from 110 to 250 °C by 2 °C/min, maintaining the temperature for 2 h, and from 250 to 400 °C, and maintaining the temperature for 6 h. For the closed form of ZSM-22, the final temperature in the activation procedure was 230 °C to avoid the loss of the organic template. The loss of the template was monitored by periodically measuring linear alkane adsorption on the closed material. Helium was used as carrier gas. The carrier gas flow rate was 20 mL/min for open ZSM-22 and for closed ZSM-22 it varied from 5 to 15 mL/min depending on the temperature and the hydrocarbon of interest. The flow rate was regulated by a mass flow controller at the inlet of the GC and measured with a soap-bubble meter at the detector outlet. Pressure drop over the chromatographic column was measured with a pressure transducer placed at the outlet of the mass flow controller.

The pulse chromatographic technique<sup>26</sup> was used to determine the adsorption equilibrium. The Henry constant was determined from the first moment of the response curve on the TCD detector after injection of an alkane trace. Adsorption enthalpy and entropy were obtained by fitting the temperature dependence of the Henry constant to the van't Hoff equation. The important experimental conditions of the adsorption experiments are given in Table 1.

## Results

Given the very low adsorption capacity of the closed material ( $0.16 \times 10^{-3}$  mL/g, Table 1), it can easily be overloaded in a pulse experiment. To verify if the measurements were performed at sufficiently low coverage to ensure the Henry regime, different volumes (between 0.1  $\mu\text{L}$  of liquid and 0.02  $\mu\text{L}$  of gas) of the adsorbate were injected with a syringe at the column inlet. The gas was sampled from the vapor phase in equilibrium with the liquid at room temperature in a 20 mL vial containing the adsorbate of interest. On open ZSM-22, nonlinearity between the retention time and amount injected was only observed for branched alkanes and not for linear molecules (Figure 1a,b). Injection volumes of 0.05  $\mu\text{L}$  of liquid for linear alkanes and 0.05  $\mu\text{L}$  of gas for branched ones were used on open ZSM-22. The chromatograms for both linear and branched alkanes on closed ZSM-22 showed a clear dependence of the retention time on the amount of injection. On closed ZSM-22, injection volumes of 0.1  $\mu\text{L}$  of liquid were too high for Henry type

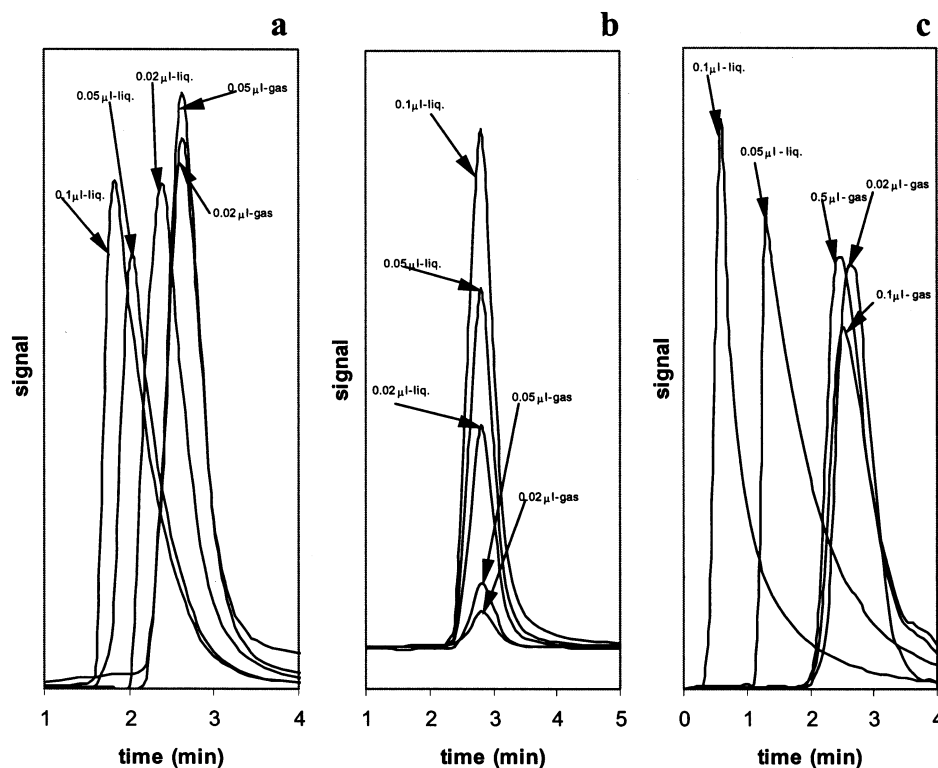


**Figure 1.** Chromatograms on both forms of ZSM-22 at 473 K showing the effect of the amount of injection on the retention times: (a) 2-methylhexane on the open form; (b) *n*-pentane on the open form; (c) 2-methylbutane on the closed form.

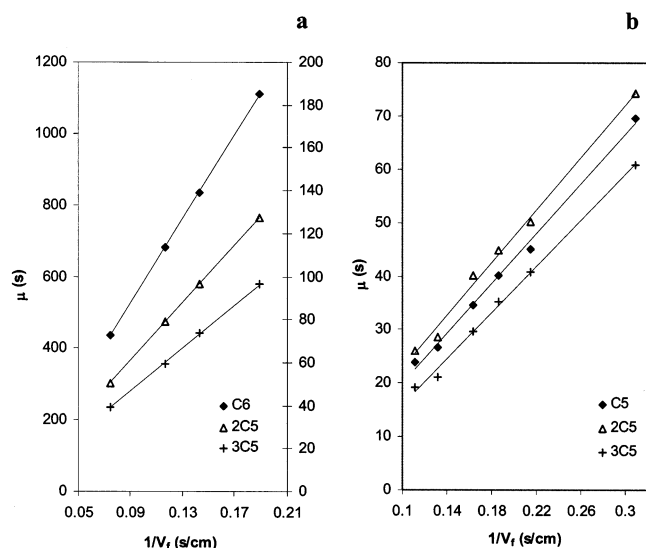


**Figure 2.** First moments with different flow rates (a) on the open ZSM-22 at 473 K (left y-axis for hexane, right y-axis for its isomers) and (b) on the closed form of ZSM-22 at 373 K.

behavior (Figure 1c), indicating that the number of adsorption sites for *n*-alkanes was dramatically reduced by closing the pores. Higher retention times were obtained with lower injection volumes and below a certain amount of injection (about 0.02  $\mu\text{L}$  of the gas phase), the change in the retention times was negligible. In all of the experiments on the closed ZSM-22, a maximum volume of 0.02  $\mu\text{L}$  of the gas was injected into the chromatographic column. The high sensitivity of the detector still allowed performing good measurements (Figure 1).

Experiments with different gas flow rates were performed to ascertain that the measurements were not affected by mass transport limitations. The retention time (first moment  $\mu$ ) of the response curve at the outlet of the column is related to the Henry

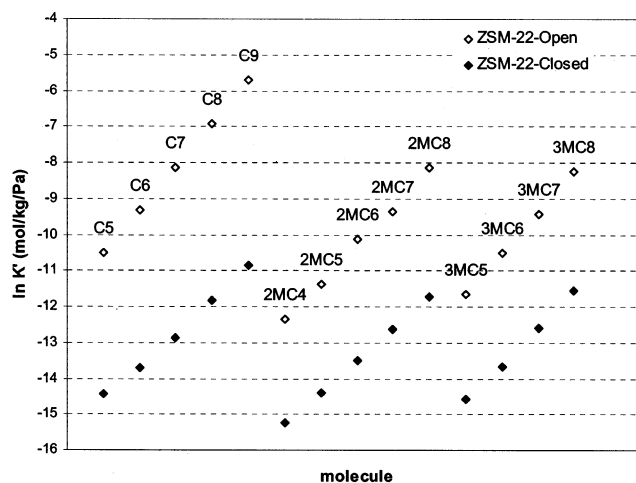


**Figure 3.** Henry constants at 473 K on both forms of ZSM-22.

constant ( $K'$ ) and the gas flow rate by

$$\mu = \frac{L}{v_f} [(\epsilon_{\text{ext}} + \epsilon_{\text{macr}}) + (1 - \epsilon_{\text{ext}} - \epsilon_{\text{macr}})RT\rho_c K'] \quad (1)$$

in which  $L$  represents the column length,  $v_f$  is the superficial gas velocity,  $\epsilon_{\text{ext}}$  and  $\epsilon_{\text{macr}}$  are the external porosity and the porosity in macropores,  $R$  is the gas constant,  $T$  is the temperature, and  $\rho_c$  is the crystal density, which was calculated assuming an ideal crystal structure.<sup>26</sup> According to this equation, a plot of the retention time versus  $1/v_f$  should yield a straight line; i.e., the Henry constants should not be dependent on the flow rate. This linearity was checked for both linear and branched alkanes by varying the flow rate from 5 to 15 mL/min for the closed form and from 7.5 to 20 mL/min for the open form. Sufficient linearity was obtained in both cases,

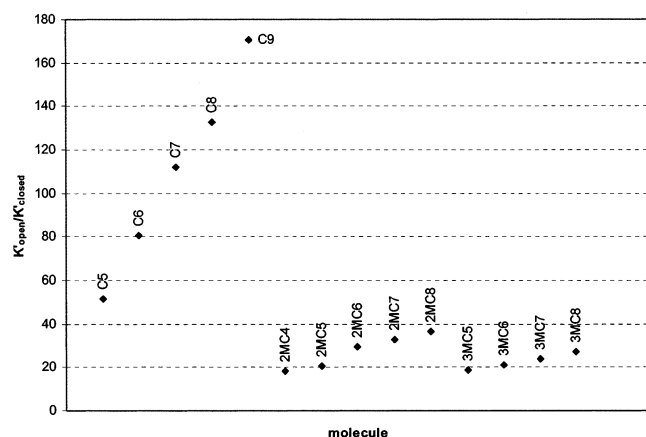
TABLE 2: Henry Adsorption Constants ( $K'$ ) on Both Forms of ZSM-22

Closed ZSM-22																			
	343 K	353 K	363 K	373 K	383 K	393 K	403 K	413 K	423 K	433 K	443 K	448 K	453 K	463 K	473 K	483 K	493 K	498 K	503 K
C5		$3.6 \times 10^{-5}$	$2.1 \times 10^{-5}$	$1.3 \times 10^{-5}$	$8.2 \times 10^{-6}$	$5.2 \times 10^{-6}$			$1.9 \times 10^{-6}$			$8.9 \times 10^{-7}$			$5.3 \times 10^{-7}$			$3.2 \times 10^{-7}$	
C6					$4.2 \times 10^{-5}$	$2.5 \times 10^{-5}$	$1.5 \times 10^{-5}$	$9.2 \times 10^{-6}$	$6.4 \times 10^{-6}$			$2.5 \times 10^{-6}$			$1.1 \times 10^{-6}$			$6.1 \times 10^{-7}$	
C7								$4.0 \times 10^{-5}$	$2.3 \times 10^{-5}$	$1.4 \times 10^{-5}$	$8.7 \times 10^{-6}$	$7.9 \times 10^{-6}$	$5.7 \times 10^{-6}$		$2.6 \times 10^{-6}$			$1.2 \times 10^{-6}$	
C8										$4.9 \times 10^{-5}$	$3.2 \times 10^{-5}$	$2.7 \times 10^{-5}$	$1.9 \times 10^{-5}$	$1.2 \times 10^{-5}$	$7.3 \times 10^{-6}$	$4.8 \times 10^{-6}$		$2.8 \times 10^{-6}$	
C9													$5.7 \times 10^{-5}$	$3.3 \times 10^{-5}$	$2.0 \times 10^{-5}$	$1.2 \times 10^{-5}$	$7.4 \times 10^{-6}$	$6.0 \times 10^{-6}$	$5.1 \times 10^{-6}$
2MC4	$2.6 \times 10^{-5}$	$1.5 \times 10^{-5}$	$9.1 \times 10^{-6}$	$5.8 \times 10^{-6}$	$3.8 \times 10^{-6}$				$1.1 \times 10^{-6}$										
2MC5				$3.3 \times 10^{-5}$	$1.9 \times 10^{-5}$	$1.2 \times 10^{-5}$	$7.2 \times 10^{-6}$		$3.2 \times 10^{-6}$			$1.4 \times 10^{-6}$							
2MC6							$3.4 \times 10^{-5}$	$2.1 \times 10^{-5}$	$1.2 \times 10^{-5}$			$3.7 \times 10^{-6}$			$1.4 \times 10^{-6}$			$6.3 \times 10^{-7}$	
2MC7										$2.2 \times 10^{-5}$	$1.3 \times 10^{-5}$	$1.2 \times 10^{-5}$	$8.0 \times 10^{-6}$	$4.9 \times 10^{-6}$	$3.2 \times 10^{-6}$			$1.2 \times 10^{-6}$	
2MC8									$1.6 \times 10^{-4}$		$3.9 \times 10^{-5}$	$2.7 \times 10^{-5}$	$2.2 \times 10^{-5}$	$1.2 \times 10^{-5}$	$8.0 \times 10^{-6}$			$2.8 \times 10^{-6}$	
3MC5				$2.5 \times 10^{-5}$	$1.4 \times 10^{-5}$	$8.8 \times 10^{-6}$			$2.5 \times 10^{-6}$			$1.1 \times 10^{-6}$							
3MC6							$1.2 \times 10^{-5}$	$6.8 \times 10^{-6}$	$4.1 \times 10^{-6}$			$1.4 \times 10^{-6}$			$1.1 \times 10^{-6}$			$2.1 \times 10^{-7}$	
3MC7									$4.0 \times 10^{-5}$			$1.0 \times 10^{-5}$			$3.4 \times 10^{-6}$			$1.1 \times 10^{-6}$	
3MC8									$1.9 \times 10^{-4}$			$3.8 \times 10^{-5}$			$9.7 \times 10^{-6}$			$3.5 \times 10^{-6}$	
Open ZSM-22																			
	333 K <sup>a</sup>	333 K <sup>b</sup>	473 K	498 K	523 K	548 K	573 K	573 K <sup>c</sup>	573 K <sup>d</sup>	598 K	623 K								
C5	$2.3 \times 10^{-2}$	$3.7 \times 10^{-2}$	$2.7 \times 10^{-5}$	$1.1 \times 10^{-5}$	$5.4 \times 10^{-6}$	$2.8 \times 10^{-6}$	$1.6 \times 10^{-6}$	$1.3 \times 10^{-6}$	$6.5 \times 10^{-7}$										
C6	$3.4 \times 10^{-1}$	$2.6 \times 10^{-1}$	$3.1 \times 10^{-5}$	$3.3 \times 10^{-5}$	$1.3 \times 10^{-5}$	$6.0 \times 10^{-6}$	$3.0 \times 10^{-6}$	$2.6 \times 10^{-6}$	$1.4 \times 10^{-6}$										
C7			$2.9 \times 10^{-4}$	$8.9 \times 10^{-5}$	$3.2 \times 10^{-5}$	$1.2 \times 10^{-5}$	$5.5 \times 10^{-6}$	$4.7 \times 10^{-6}$	$2.8 \times 10^{-6}$										
C8					$8.7 \times 10^{-5}$	$2.9 \times 10^{-5}$	$1.1 \times 10^{-5}$			$4.5 \times 10^{-6}$	$2.1 \times 10^{-6}$								
C9					$1.9 \times 10^{-4}$	$5.8 \times 10^{-5}$	$1.9 \times 10^{-5}$			$7.7 \times 10^{-6}$	$2.9 \times 10^{-6}$								
2MC4	$6.8 \times 10^{-4}$	$1.9 \times 10^{-4}$	$4.3 \times 10^{-6}$	$2.1 \times 10^{-6}$	$1.2 \times 10^{-6}$	$7.7 \times 10^{-7}$	$4.7 \times 10^{-7}$	$3.2 \times 10^{-7}$	$1.2 \times 10^{-7}$										
2MC5	$8.6 \times 10^{-3}$	$2.0 \times 10^{-3}$	$1.2 \times 10^{-5}$	$4.9 \times 10^{-6}$	$2.4 \times 10^{-6}$	$1.3 \times 10^{-6}$	$8.1 \times 10^{-7}$	$5.4 \times 10^{-7}$	$2.3 \times 10^{-7}$										
2MC6			$4.1 \times 10^{-5}$	$1.4 \times 10^{-5}$	$5.9 \times 10^{-6}$	$2.6 \times 10^{-6}$	$1.4 \times 10^{-6}$	$1.1 \times 10^{-6}$	$6.7 \times 10^{-7}$										
2MC7			$1.0 \times 10^{-4}$	$3.4 \times 10^{-5}$	$1.2 \times 10^{-5}$	$5.0 \times 10^{-6}$	$2.2 \times 10^{-6}$												
2MC8			$2.9 \times 10^{-4}$	$8.1 \times 10^{-5}$	$2.6 \times 10^{-5}$	$9.3 \times 10^{-6}$	$3.8 \times 10^{-6}$												
3MC5			$8.8 \times 10^{-6}$	$4.0 \times 10^{-6}$	$2.1 \times 10^{-6}$	$1.1 \times 10^{-6}$	$6.2 \times 10^{-7}$	$4.4 \times 10^{-7}$	$1.8 \times 10^{-7}$										
3MC6			$2.7 \times 10^{-5}$	$1.1 \times 10^{-5}$	$4.3 \times 10^{-6}$	$2.0 \times 10^{-6}$	$1.1 \times 10^{-6}$	$8.7 \times 10^{-7}$	$3.4 \times 10^{-7}$										
3MC7			$8.2 \times 10^{-5}$	$2.5 \times 10^{-5}$	$9.5 \times 10^{-6}$	$4.1 \times 10^{-6}$	$1.9 \times 10^{-6}$												
3MC8			$2.7 \times 10^{-4}$	$7.1 \times 10^{-5}$	$2.3 \times 10^{-5}$	$8.3 \times 10^{-6}$	$3.5 \times 10^{-6}$												

<sup>a</sup> Extrapolated to 333 K using the van't Hoff relation. <sup>b</sup> Measured with the calorimetric technique.<sup>27</sup> <sup>c</sup> Measured chromatographically.<sup>24</sup> <sup>d</sup> Calculated using the configurational-bias Monte Carlo technique.<sup>15</sup>

**TABLE 3: Coefficients  $A$  and  $B$  of the Correlation  $K' = Ae^{BCN}$  between Henry Constants and Carbon Number for the Linear, 2- and 3-Methyl-Branched Alkanes at 473 K**

	$A$			$B$		
	linear	2-Me branched	3-Me branched	linear	2-Me branched	3-Me branched
open ZSM-22	$6.7 \times 10^{-8}$	$2.1 \times 10^{-8}$	$9.7 \times 10^{-9}$	1.2	1.06	1.13
closed ZSM-22	$5.1 \times 10^{-9}$	$3.0 \times 10^{-9}$	$4.8 \times 10^{-10}$	0.909	0.875	1.09

**Figure 4.** Ratio of Henry constants at 473 K of the open over the closed forms of ZSM-22.

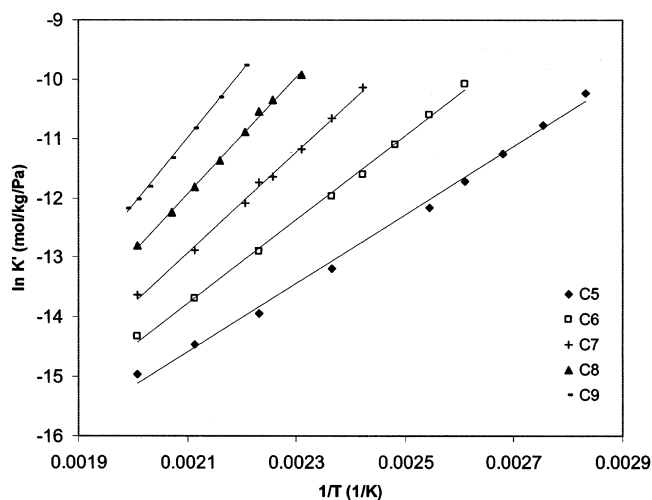
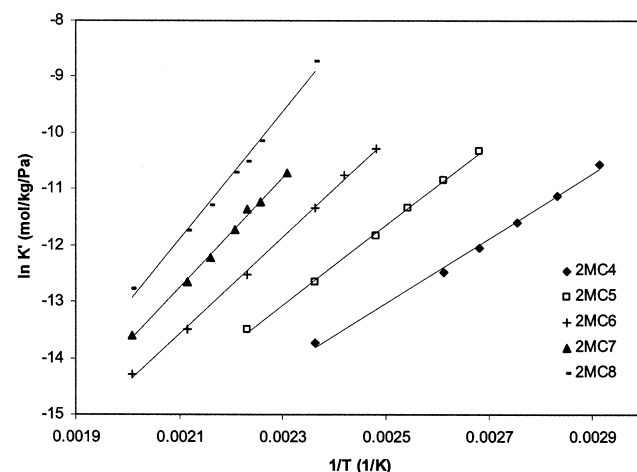
demonstrating that even for the more bulky isomers no diffusion limitations occurred under the experimental conditions (Figure 2).

**Henry Constants.** The Henry adsorption constants ( $K'$ ) of the linear and 2- and 3-methyl-branched alkanes on both forms of ZSM-22 at 473 K are plotted in Figure 3, and all  $K'$  values are summarized in Table 2 together with the data found in the literature. Our data are in good agreement with the scarce data obtained with different techniques such as calorimetry and molecular simulation. On both types of ZSM-22, the Henry constants increase exponentially with the carbon number for linear as well as for branched alkanes, typically found for adsorption of homologous series of hydrocarbon molecules on microporous materials.<sup>27–29</sup> The carbon number dependence can be represented by the equation

$$K' = Ae^{BCN} \quad (2)$$

This exponential increase is explained by the incremental character of the enthalpy and entropy contributions depending on the number of methyl groups in the alkane chain.<sup>24</sup> These temperature dependent parameters  $A$  and  $B$  are related to the adsorption enthalpy and entropy and depend strongly on the zeolite type and pore size (Table 3).<sup>24</sup>

The narrow pore structure of TON exhibits strong shape selectivity between linear and branched alkanes. As already observed before,<sup>24,30</sup> the Henry constants of the branched alkanes are significantly lower than those of the linear alkanes on the open form of ZSM-22 (Table 2). On the closed form, the differences in Henry constants between linear and mono-branched alkanes are much less pronounced. The Henry constant at 473 K of, e.g., heptane is 7 times larger than its isomer 2-methylhexane on the open form, where it is only about 2 times larger on the closed form. The Henry constants of the 3-methyl isomers are comparable to the 2-methyl isomers on the closed form, whereas on the open form the latter are somewhat higher than the former (Table 2). Figure 4 represents the ratio of  $K'$  values on the open over the closed forms of ZSM-22. Closing of the pores has the strongest impact on the  $K'$  values of the  $n$ -alkanes: the  $K'$  value of  $n$ -heptane at 473 K is 112 times

**Figure 5.** van't Hoff plot of  $n$ -alkanes on the closed form of ZSM-22.**Figure 6.** van't Hoff plot of 2-methyl-branched alkanes on the closed form of ZSM-22.

larger on open ZSM-22 compared to closed ZSM-22. For branched compounds such as 2-methylhexane, this ratio is much lower and amounts only to 29.

**Adsorption Enthalpy.** The adsorption enthalpies ( $\Delta H_0$ ) were derived from the temperature dependence of the Henry constants by linear regression of the experimental data using the van't Hoff equation:

$$K' = K'_0 e^{-\Delta H_0/RT} \quad (3)$$

The van't Hoff plots on closed ZSM-22 are given in Figures 5–7. The plots are linear over the whole temperature range. The upper bound of the investigated temperature range differed from one component to another and was limited by the accurate determination of the relatively short retention times on the closed form. The adsorption enthalpies and preexponential factors of the van't Hoff equation are summarized in Table 4 for both forms of ZSM-22 together with literature values for comparison. The values on the open form are in good agreement with



TABLE 4: Adsorption Enthalpies and Pre-exponential Factors on Both Forms of ZSM-22

	$-\Delta H_0$ (kJ/mol)			$K_0'$ (mol/kg/Pa)	
	open ZSM-22	literature		open ZSM-22	closed ZSM-22
<i>n</i> -pentane	63.3 ± 1.6	62, <sup>a</sup> 71 <sup>b</sup>	47.7 ± 1.2	$2.7 \times 10^{-12} \pm 1.5$	$2.7 \times 10^{-12} \pm 1.4$
<i>n</i> -hexane	77.1 ± 0.9	74.5, <sup>a</sup> 81.5, <sup>b</sup> 72.3 <sup>d</sup>	58.5 ± 1.1	$2.7 \times 10^{-13} \pm 1.2$	$4.0 \times 10^{-13} \pm 1.4$
<i>n</i> -heptane	89.4 ± 0.7	85.9, <sup>a</sup> 104 <sup>c</sup>	70.9 ± 1.6	$3.7 \times 10^{-14} \pm 1.2$	$4.1 \times 10^{-14} \pm 1.5$
<i>n</i> -octane	100.6 ± 1.3		81.7 ± 1.6	$7.5 \times 10^{-15} \pm 1.3$	$7.3 \times 10^{-15} \pm 1.5$
<i>n</i> -nonane	112.5 ± 0.9		92.7 ± 1.3	$1.3 \times 10^{-15} \pm 1.2$	$1.2 \times 10^{-15} \pm 1.4$
2-methylbutane	49.3 ± 1.3	59.8, <sup>a</sup> 47.5 <sup>b</sup>	47.7 ± 1.6	$1.5 \times 10^{-11} \pm 1.4$	$1.3 \times 10^{-12} \pm 1.7$
2-methylpentane	60.0 ± 1.9	69.9, <sup>a</sup> 59 <sup>b</sup>	59.1 ± 1.2	$2.6 \times 10^{-12} \pm 1.5$	$1.7 \times 10^{-13} \pm 1.4$
2-methylhexane	76.1 ± 1.7	84.6, <sup>a</sup> 93.4 <sup>c</sup>	71.1 ± 1.4	$1.5 \times 10^{-13} \pm 1.5$	$2.0 \times 10^{-14} \pm 1.5$
2-methylheptane	87.3 ± 1.3		81.0 ± 2.0	$2.4 \times 10^{-14} \pm 1.1$	$3.7 \times 10^{-15} \pm 1.7$
2-methyloctane	97.8 ± 0.9		93.7 ± 3.8	$4.5 \times 10^{-15} \pm 1.2$	$3.6 \times 10^{-16} \pm 2.7$
3-methylpentane	59.4 ± 0.4	69.9 <sup>a</sup>	57.2 ± 1.5	$2.4 \times 10^{-12} \pm 1.1$	$2.3 \times 10^{-13} \pm 1.6$
3-methylhexane	72.0 ± 1.7	81.4, <sup>a</sup> 84.7 <sup>c</sup>	69.9 ± 0.7	$3.0 \times 10^{-13} \pm 1.5$	$1.0 \times 10^{-14} \pm 1.2$
3-methylheptane	84.5 ± 1.5		83.2 ± 1.1	$3.6 \times 10^{-14} \pm 1.4$	$2.2 \times 10^{-15} \pm 1.3$
3-methyloctane	97.8 ± 1.3		93.6 ± 3.2	$4.0 \times 10^{-15} \pm 1.4$	$4.9 \times 10^{-16} \pm 2.3$

<sup>a</sup> From ref 15. <sup>b</sup> From ref 27. <sup>c</sup> From ref 8. <sup>d</sup> From ref 22.

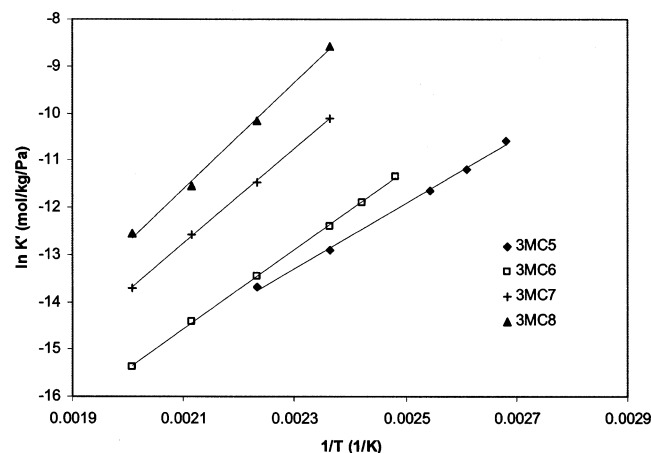


Figure 7. van't Hoff plot of 3-methyl-branched alkanes on the closed form of ZSM-22.

previously reported data (Table 4). A remarkable observation is that the van't Hoff plot of 3-methylpentane does not follow the trend obtained with the other 3-methyl-branched molecules. The measured  $K'$  values are almost as high as those of 3-methylhexane (see Figure 7). However, the slope of the van't Hoff plot (adsorption enthalpy) of this molecule shows a normal behavior (Table 4). We believe the symmetry of 3-methylpentane is at the basis of the relatively high Henry adsorption constants.

Adsorption enthalpies of linear and 2-methyl- and 3-methyl-branched alkanes are plotted in Figure 8. A linear relationship between carbon number and adsorption enthalpy is found for open as well as closed ZSM-22. An increment of about 12 kJ/mol per added carbon is observed for linear and 2- and 3-methyl-branched alkanes on the open form. This increment was about 11 kJ/mol on the closed form. On the open form of ZSM-22, 2-methyl-branched alkanes showed about 13–17 kJ/mol lower values for the adsorption enthalpy than the values determined for the corresponding *n*-alkanes, whereas 3-methyl-branched alkanes have an adsorption enthalpy, which is 15–18 kJ lower than those of the linear chains (Table 4). Eder et al.<sup>27</sup> reported a lowering of the adsorption enthalpy of 12.5 kJ/mol from *n*-butane to isobutane and 12 kJ/mol from *n*-pentane to isopentane.

The differences in adsorption enthalpy between the open and closed form of ZSM-22 for all studied molecules are represented in Figure 9. The adsorption enthalpies of linear alkanes are much higher (16–20 kJ/mol) on the open form than on the closed

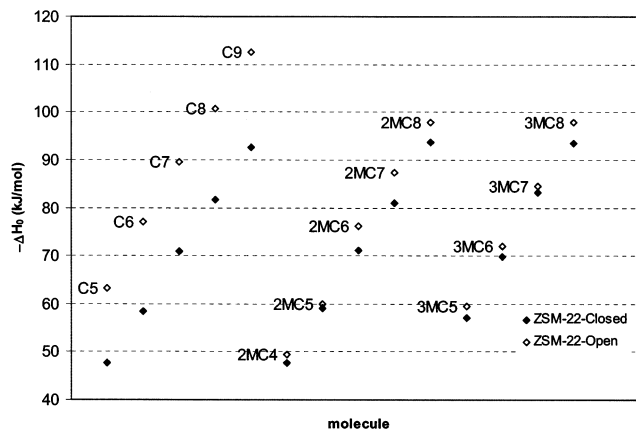


Figure 8. Low coverage adsorption enthalpies ( $-\Delta H_0$ ) on both forms of ZSM-22.

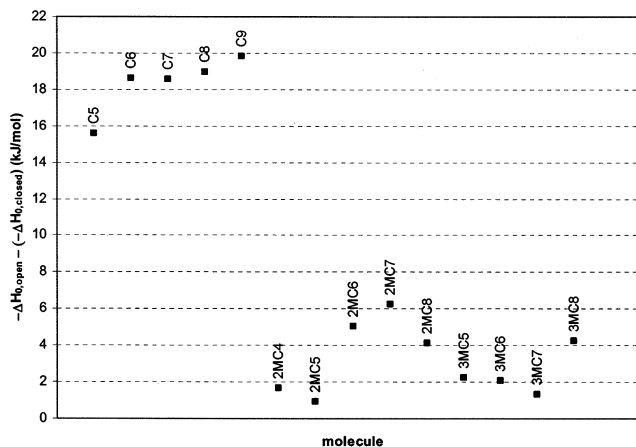
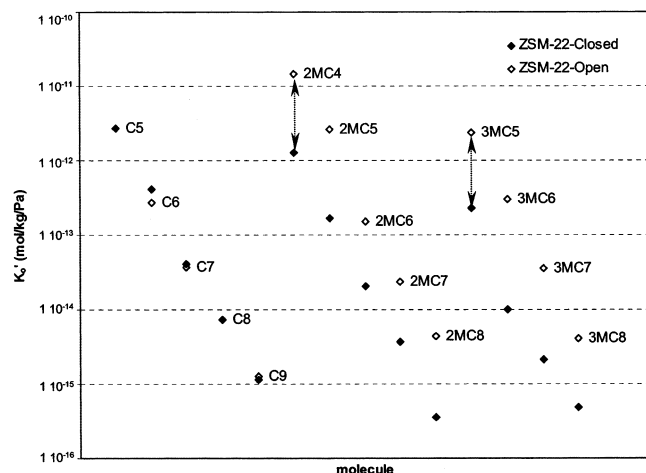


Figure 9. Differences in adsorption enthalpies between the open and closed forms of ZSM-22.

form but only slight differences (1–6 kJ/mol) are observed for the branched molecules (Table 4).

**Entropy of Adsorption.** The preexponential factors ( $K_0'$ ) of the van't Hoff equation are given in Figure 10 and Table 4 for open and closed forms of ZSM-22. The preexponential factors decrease exponentially with the carbon number for all alkane isomer families (Figure 10). On the open ZSM-22, the preexponential factors of the branched alkanes are up to 1 order of magnitude higher than those of the linear chains. On the closed form, however, the branched alkanes have a 2–4 times lower preexponential factor than the linear alkanes.



**Figure 10.** Preexponential factors on both forms of ZSM-22. The arrows indicate corresponding open-closed values.

The preexponential factor  $K_0'$  of the van't Hoff equation (eq 3) is associated with the adsorption entropy  $\Delta S_{0,\text{local}}^\ominus$  and the number of adsorption sites  $n_T$  as

$$K_0' = \exp \left[ \frac{\Delta S_{0,\text{local}}^\ominus}{R} + \ln \left( \frac{n_T}{2p^\ominus} \right) \right] \quad (4)$$

in which  $p^\ominus$  is the standard pressure chosen as 0.1 MPa.<sup>24,25</sup>

In regard to the very small Henry constants ( $K'$ ) and micropore volume (Table 1) of the closed form, it can well be assumed that the number of adsorption sites ( $n_T$ ) is much smaller on the closed form when compared with the open form. Thus, this decrease in  $n_T$  should result in lower preexponential factors ( $K_0'$ ), which is the case for branched alkanes where a drop of 1 order of magnitude is observed (Figure 10). Interestingly, for linear alkanes, the preexponential factors remain unaltered on the closed ZSM-22. This observation can than only be explained by a compensating change in the adsorption entropy as discussed further.

## Discussion

The present experimental adsorption data cannot be explained by a classic intracrystalline adsorption model but can be reconciled using a pore mouth adsorption model. It is observed that Henry constants of linear alkanes decrease drastically when the pores of ZSM-22 are closed, whereas this effect is much less pronounced for branched alkanes (Figure 4). This observation suggests that the interaction of linear and monobranched alkanes with open ZSM-22 must be of a different nature.

Adsorption enthalpies of linear alkanes on open ZSM-22 are 13–17 kJ/mol higher than those of the isomers with the methyl group in position 2, and 15–18 kJ/mol higher than those of the isomers with the methyl side branch in position 3 (Table 4). The increase of adsorption enthalpy per added  $\text{CH}_2$  group is the same for linear and monobranched alkanes. In the adsorption of saturated hydrocarbons, dispersion-repulsion forces prevail, owing to their apolar character. Eder et al.<sup>27</sup> studied the role of pore size in the adsorption of linear and branched alkanes and concluded that the adsorption enthalpy depends subtly on the agreement between the size of the alkane molecule and the size of the zeolite pores. This can be seen in Figure 11 where adsorption enthalpies of *n*-heptane and 2- and 3-methylhexane are compiled for various zeolites with different pore sizes. From zeolite Y to ZSM-22 a decrease from 1.3 to 0.5 nm in pore diameter is accompanied by an increase of 37 kJ/mol (from 51.9

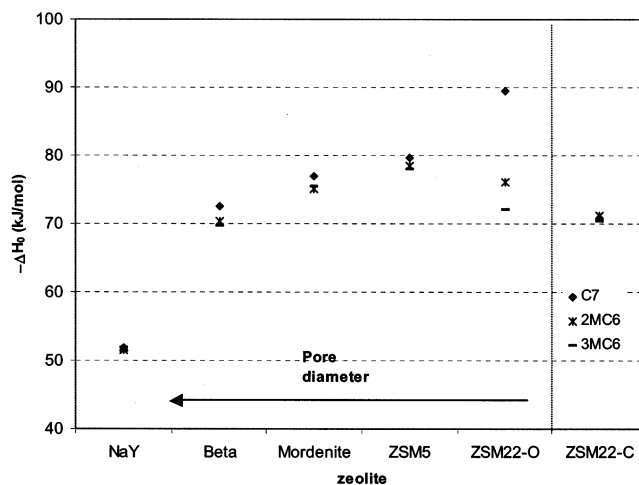


**Figure 11.** Adsorption enthalpies of *n*-heptane and its isomers on different zeolites. (Data for NaY, beta, mordenite and ZSM-5 are taken from ref 24).

kJ/mol for NaY to 89.4 kJ/mol for ZSM-22) in the adsorption enthalpy for *n*-heptane (Figure 11). On the other hand, the relationship between the adsorption enthalpy and pore size is different for monobranched alkanes. For 2- and 3-methyl-branched alkanes the adsorption enthalpy increases from zeolite Y to ZSM-5 but decreases again in ZSM-22 (Figure 11). The lower adsorption enthalpy in ZSM-22 can be due to repulsion,<sup>27</sup> or to adsorption in pore mouths, with the molecule partly inside and partly outside the pore.

When the pores are closed, an important decrease in adsorption enthalpy is observed for linear alkanes, because they are no longer allowed to adsorb in the high interaction region inside the ZSM-22 channels (Figure 9 and Table 4). The difference in *n*-alkane adsorption enthalpy between open and closed ZSM-22 becomes larger with increasing chain length: 15.6 kJ/mol for *n*-pentane and 19.8 kJ/mol for *n*-nonane (Table 4). In accordance with the pore mouth model, the effect of closing the pores on the adsorption of branched alkanes is very limited and also becomes more important at higher chain lengths (1.7 kJ/mol for 2-methylbutane, 4.1 kJ/mol for 2-methyloctane). On the closed form the adsorption enthalpies of linear and 2-methyl- and 3-methyl-branched isomers are close to each other because all these molecules are now adsorbed on the same sites, viz. pore mouths (Figure 8). The adsorption enthalpies observed on closed ZSM-22 are larger than on a large pore zeolite such as zeolite Y (Figure 11). It implies that on closed ZSM-22, both parts of the molecule inside and outside the pore can interact very favorably with the zeolite, the pore mouth and the external surface, respectively. In closed ZSM-22, the micropore volume according to nitrogen adsorption is extremely small ( $0.16 \times 10^{-3}$  mL/g, Table 1); hence the free depth of evacuated pore mouths is very limited. Considering a distribution of such partially blocked pore mouths with various "adsorption depths", it can be understood that the differences between the open and the closed form become larger with increasing chain length (Figure 9).

The influence of closing pores on the preexponential factors of the van't Hoff equation can also be explained on the basis of the pore mouth model. For branched alkanes, the number of adsorption sites  $n_T$  equals the number of pore mouths, which has been estimated as  $3.4 \times 10^{-7}$  mol/g on open ZSM-22.<sup>25</sup> For the linear alkanes, it can be reasonably accepted that  $n_T$  equals the number of Brønsted acid sites. The number of Brønsted acid sites calculated using the structure formula of

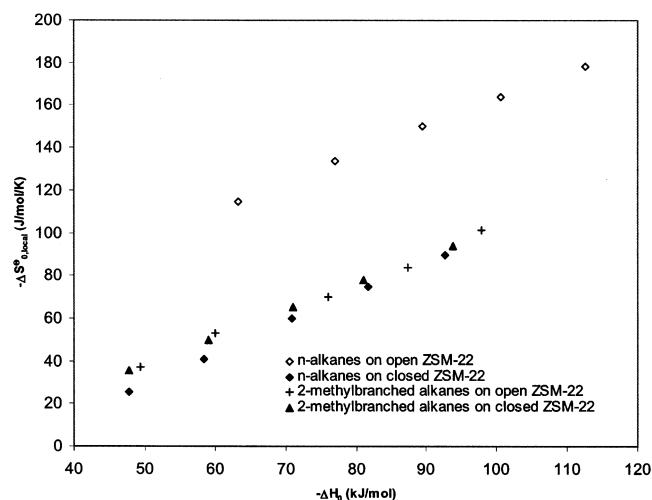


**Figure 12.** Compensation chart for linear and 2-methyl-branched alkanes.

**TABLE 5: Calculated Entropies of Adsorption for Linear and 2-Methyl-Branch Alkanes**

	$-\Delta S_{0,\text{local}}^{\ominus}$ [J/(mol K)]	
	open ZSM-22	closed ZSM-22
<i>n</i> -pentane	115	25
<i>n</i> -hexane	134	41
<i>n</i> -heptane	150	60
<i>n</i> -octane	164	75
<i>n</i> -nonane	179	90
2-methylbutane	37	35
2-methylpentane	53	50
2-methylhexane	70	65
2-methylheptane	84	78
2-methyloctane	102	94

TON is  $0.54 \cdot 10^{-3}$  mol/g. With this information, the entropy of adsorption of linear and branched alkanes on open ZSM-22 can be calculated using eq 4. The calculated values for linear and 2-methyl-branched alkanes are given in Table 5. An increase of 16 J/(mol K) per added carbon is observed for both linear and the branched hydrocarbons. This value is in good agreement with 15 J/(mol K) that was previously reported.<sup>31</sup> In Figure 12, the adsorption entropy is plotted as a function of the adsorption enthalpy, indicating a linear relationship between these two thermodynamic properties, as already observed by several authors. This effect is known as the iso-equilibrium or compensation effect.<sup>32–36</sup>

For the closed ZSM-22, the adsorption entropies cannot be calculated directly, because the number of accessible pore mouths is unknown. Taking into account that adsorption enthalpies of the branched alkanes are comparable on the closed and open ZSM-22 samples (Table 4), it can be accepted that the nature of the adsorption sites is the same on both materials. Hence, the adsorption entropy of the branched alkanes on the closed ZSM-22 can be calculated using the correlation between adsorption enthalpy and entropy found on the open ZSM-22 for branched alkane molecules (Figure 12).

Using the calculated adsorption entropies together with the experimentally determined preexponential factors of the branched alkanes, the number of accessible pore mouths on the closed ZSM-22 is calculated by using eq 4 and corresponds to approximately 3% of the number of pore mouths on the open form. As the number of adsorption sites for linear alkanes equals the number of accessible pore mouths on the closed ZSM-22, the adsorption entropies of the linear alkanes on the closed form can be calculated using the same equation (Table 5). Whereas

**TABLE 6: Slopes of the Lines on the Compensation Chart**

	slope
<i>n</i> -alkanes (open ZSM-22)	1.29
<i>n</i> -alkanes (closed ZSM-22)	1.44
2-methyl-branched alkanes (open ZSM-22)	1.30
2-methyl-branched alkanes (closed ZSM-22)	1.47

the entropies and enthalpies of adsorption of the branched molecules are not affected by closing the pores, a significant drop in both the adsorption enthalpy (e.g., from 101 to 82 kJ/mol for *n*-octane) and entropy (e.g., from 164 to 87 J/mol K for *n*-octane) is observed for the linear alkanes (Tables 4 and 5).

A very interesting result is obtained when the entropies are plotted as a function of the adsorption enthalpy for both materials (Figure 12). For the adsorption of *n*-alkanes on the open ZSM-22, much higher adsorption entropies are obtained than for the branched alkanes for the same adsorption enthalpy. *n*-Alkanes are confined inside the narrow ZSM-22 channels, where they lose more degrees of freedom compared to the branched alkanes, located in the relatively open pore mouths. The most remarkable observation is that the data points for adsorption of *n*-alkanes on the closed ZSM-22 coincide with the curve of the branched alkanes (Figure 12). The observation that linear alkanes behave thermodynamically identical as branched alkanes on a ZSM-22 in which the channels were blocked gives solid evidence for the pore mouth theory. *n*-Alkanes forced to adsorb in the pore mouths retain much more freedom than alkanes inside the pores. However, on an open ZSM-22, it is more favorable for linear alkanes to adsorb inside the pore as a result of the much higher energetic interaction and the higher number of adsorption sites.

Table 6 gives the variation of  $-\Delta S_{0,\text{local}}^{\ominus}$  with  $-\Delta H_0$  for the open and closed ZSM-22. The entropy increases more rapidly with the adsorption enthalpy for adsorption in pore mouths than for adsorption inside the pore. This is explained by the fact that small molecules residing in the pore mouth retain much more freedom compared to small molecules inside the pore but with increasing chain length, additional CH<sub>2</sub> groups stick inside the pores resulting in an important increase in the adsorption enthalpy.

## Conclusions

Using the tracer chromatographic technique, reliable Henry constants and adsorption enthalpies and entropies of C<sub>5</sub>–C<sub>9</sub> *n*-alkanes and their isomers were determined on open ZSM-22 and closed ZSM-22. The adsorption of linear alkanes is strongly affected by the blocking of the pores, whereas the adsorption of monobranched alkanes is altered very little. These observations are in agreement with a pore mouth adsorption model for monobranched isoalkanes. According to this model, branched alkanes stick with their longest linear alkyl group inside a ZSM-22 pore, whereas the tertiary carbon atom together with its two other, shorter *n*-alkyl substituents remains outside. Linear alkanes have free access to the micropores. Branched molecules adsorbed in pore mouths retain much more freedom, as reflected in the much smaller adsorption entropies. Linear molecules adsorbed on the pore mouths show the same relation between entropy and enthalpy of adsorption as branched molecules.

**Acknowledgment.** This research was financially supported by FWO Vlaanderen (G.0127.99). J.D. is grateful to the F.W.O.-Vlaanderen, for a fellowship as a postdoctoral researcher. The involved teams are participating in the IAP-PAI programme



(IUAP IV-11) on Supramolecular Chemistry and Catalysis, sponsored by the Belgian Federal Government.

## References and Notes

- (1) Souverijns, W.; Martens, J. A.; Froment, G. F.; Jacobs, P. A. *J. Catal.* **1998**, *174*, 177.
- (2) Martens, J. A.; Parton, R.; Uytterhoeven, L.; Jacobs, P. A. *Appl. Catal.* **1991**, *76*, 95.
- (3) Clet, G.; Goupil, J. M.; Szabo, G.; Cornet, D. *Appl. Catal. A: General* **2000**, *202*, 37.
- (4) Duchet, J. C.; Guillaume, D.; Monnier, A.; Dujardin, C.; Gilson, J. P.; van Gestel, J.; Szabo, G.; Nascimento, P. J. *Catal.* **2001**, *198*, 328.
- (5) Liu, H.; Lei, G. D.; Sachtler, W. M. H. *Appl. Catal. A: General* **1996**, *137*, 167.
- (6) Xiao, S.; Mao, R. L. V. *Micropor. Mater.* **1995**, *4*, 435.
- (7) Baltanas, M. A.; van Raemdonck, K. K.; Froment, G. F.; Mohedas, S. R. *Ind. Eng. Chem. Res.* **1989**, *28*, 899.
- (8) Raybaud, P.; Patriceon, A.; Toulhoat, H. *J. Catal.* **2001**, *197*, 98.
- (9) Aoki, K.; Kusakabe, K.; Morooka, S. *Ind. Eng. Chem. Res.* **2000**, *39*, 2245.
- (10) Silva, J. A. C.; da Silva, F. A.; Rodrigues, A. E. *Sep. Purif. Technol.* **2000**, *20*, 97.
- (11) Babich, I. V.; van Langeveld, A. D.; Zhu, W. D.; Bakker, W. J. W.; Moulijn, J. A. *Ind. Eng. Chem. Res.* **2001**, *40*, 357.
- (12) Parton, R.; Uytterhoeven, L.; Martens, J. A.; Jacobs, P. A. *Appl. Catal.* **1991**, *76*, 131.
- (13) Ernst, S.; Weitkamp, J.; Martens, J. A.; Jacobs, P. A. *Appl. Catal.* **1989**, *48*, 137.
- (14) Webb, E. B., III; Grest, G. S. *Catal. Lett.* **1998**, *56*, 95.
- (15) Maesen, Th. L. M.; Schenk, M.; Vlucht, T. J. H.; de Jonge, J. P.; Smit, B. *J. Catal.* **1999**, *188*, 403.
- (16) Sastre, G.; Chica, A.; Corma, A. *J. Catal.* **2000**, *195*, 227.
- (17) Claude, M. C.; Vanbutsele, G.; Martens, J. A. *J. Catal.* **2001**, *203*, 213.
- (18) Souverijns, W.; Martens, J. A.; Uytterhoeven, L.; Froment, G. F.; Jacobs, P. A. *Prog. Zeolite Micropor. Mater.* **1997**, *105*, 1285.
- (19) Pieterse, J. A. Z.; Veeffkind-Reyes, S.; Seshan, K.; Lercher, J. A. *J. Phys. Chem. B* **2000**, *104*, 5715.
- (20) Choudhary, V. R.; Singh, A. P.; Kumar, R. *J. Catal.* **1991**, *129*, 293.
- (21) Webb, E. B., III; Grest, G. S.; Mondello, M. *J. Phys. Chem. B* **1999**, *103*, 4949.
- (22) Anderson, B. G.; de Gauw, F. J. M. M.; Noordhoek, N. J.; van Ijzendoorn, L. J.; van Santen, R. A.; de Voigt, M. J. A. *Ind. Eng. Chem. Res.* **1998**, *37*, 815.
- (23) Noordhoek, N. J.; van Ijzendoorn, L. J.; Anderson, B. G.; de Gauw, F. J.; van Santen, R. A.; de Voigt, M. J. *Ind. Eng. Chem. Res.* **1998**, *37*, 825.
- (24) Denayer, J. F.; Souverijns, W.; Jacobs, P. A.; Martens, J. A.; Baron, G. V. *J. Phys. Chem. B* **1998**, *102*, 4588.
- (25) Martens, J. A.; Vanbutsele, G.; Jacobs, P. A.; Denayer, J.; Ocakoglu, R.; Baron, G.; Munoz Arroyo, J. A.; Thybaut, J.; Marin, G. B. *Catal. Today* **2001**, *65*, 111.
- (26) Ruthven, D. M. *Principles of adsorption and adsorption processes*; John Wiley and Sons: New York, 1984; p 220.
- (27) Eder, F.; Lercher, J. A. *J. Phys. Chem. B* **1997**, *101*, 1273.
- (28) Nabivach, V. M.; Dmitriyev, V. P. *Russ. Chem. Rev.* **1993**, *62* (1), 23.
- (29) Smit, B.; Siepmann, J. I. *J. Phys. Chem.* **1994**, *98*, 8442.
- (30) Denayer, J. F.; Baron, G. V.; Martens, J. A. *Prepr. Topical Conf. Sep. Sci. Technol. AIChE* **1997**, 1447.
- (31) J. F. Denayer; G. V. Baron; Martens, J. A.; Jacobs, P. A. *J. Phys. Chem. B* **1998**, *102*, 3077.
- (32) Ruthven, D. M.; Kaul, B. K. *Adsorption* **1998**, *4*, 269.
- (33) Atkinson, D.; Curthoys, G. *J. Chem. Soc.* **1981**, *77*, 897.
- (34) Eder, F.; Lercher, J. A. *Zeolites* **1997**, *18*, 75.
- (35) Katsanos, N. A.; Lycourghiotis, A.; Tsiatsios, A. *J. Chem. Soc.* **1978**, *74*, 575.
- (36) Eder, F.; He, Y.; Nivarthi, G.; Lercher, J. A. *Rec. Trav. Chim. Pays-Bas* **1996**, *115*, 531.